European Journal of AI, Computing & Informatics

Article

MCATSA: Multi-Strategy Collaborative Adaptive Tree-Seed Algorithm and Its Application in Dynamic Credit Risk Assessment

Kaiyu Huang [1,*]

[1] Jilin University of Finance and Economics, Changchun, China
* Correspondence: Kaiyu Huang, Jilin University of Finance and Economics, Changchun, China

Abstract: Credit risk assessment lies at the absolute core of maintaining global financial system stability and preventing systemic economic crises. However, traditional static evaluation models increasingly suffer from significant limitations when dealing with the complexities of multi-source heterogeneous data, intricate spatiotemporal risk contagion, and the urgent need for dynamic decision-making in modern financial markets. To comprehensively address these critical issues, this paper proposes a novel integrated risk control framework, denoted as IOA-DGNN-RL. This advanced architecture is fundamentally based on a newly improved Multi-Strategy Collaborative Adaptive Tree-Seed Algorithm (MCATSA), a Dynamic Graph Neural Network (DGNN), and Reinforcement Learning (RL) techniques. Firstly, the proposed MCATSA substantially improves the standard Tree-Seed Algorithm through the integration of five core mechanisms, which include heterogeneous chaotic initialization, multi-layer resource allocation, and nonlinear energy regulation. These enhancements achieve highly accurate dimensionality reduction of high-dimensional non-financial features, thereby optimizing computational efficiency. Secondly, a sophisticated DGNN model incorporating key macroeconomic indicators is constructed to precisely capture spatiotemporal risk propagation within the complex topological network among interconnected enterprises. Finally, a robust reinforcement learning decision module is designed to seamlessly transform dynamic risk predictions into actionable, optimal credit adjustment strategies. Comprehensive experiments demonstrate that the MCATSA performs excellently in standard benchmark optimization tasks. Furthermore, the complete integrated system achieves an impressive Area Under the Curve (AUC) of 0.901 on complex real-world credit datasets, significantly outperforming existing baseline methods and providing a highly reliable tool for modern financial risk management.

Keywords: tree-seed algorithm; graph neural networks; reinforcement learning; feature selection; credit risk assessment

Received: 20 March 2026
Revised: 30 April 2026
Accepted: 13 May 2026
Published: 17 May 2026

Copyright: © 2026 by the authors. Submitted for possible open access publication under the terms and conditions of the Creative Commons Attribution (CC BY) license (https://creativecommons.org/licenses/by/4.0/).

1. Introduction

1.1. Background and Motivation

Credit risk assessment is a fundamental component of modern financial risk management, serving as a critical tool for evaluating the potential risks associated with lending and investment decisions. However, as the global economic network becomes increasingly interconnected, traditional static risk control models have demonstrated significant limitations. One major drawback is their inability to effectively capture the intricate correlation risks and contagion effects that arise among interconnected enterprises. These models often fail to account for the cascading impacts that can propagate through economic networks, leading to systemic vulnerabilities. Additionally, traditional approaches lack the capacity to adapt dynamically to changes in the macroeconomic environment, which is essential for maintaining robust risk control in the face of economic fluctuations. Consequently, there is an urgent demand for an innovative

risk assessment framework that integrates dynamic network topology analysis with macroeconomic contextual factors, enabling more accurate and adaptive decision-making in financial risk management [1].

1.2. Related Work

In recent years, swarm intelligence optimization algorithms, graph neural networks (GNNs), and reinforcement learning have gained significant traction in financial modeling due to their ability to handle complex data structures and dynamic environments. For example, Particle Swarm Optimization and Tree-Structured Search Algorithm are widely employed for feature selection tasks. However, traditional approaches often face challenges such as becoming trapped in local optima when processing high-dimensional and intricate datasets. Concurrently, static GNNs, while effective in certain contexts, lack the flexibility to capture the temporal dynamics inherent in evolving risk networks [2, 3]. This limitation restricts their application to merely predicting risks rather than enabling a comprehensive, data-driven decision-making framework. Addressing these gaps requires innovative methodologies that integrate temporal modeling capabilities and feedback mechanisms, ensuring more robust and adaptive financial risk management systems.

1.3. Contributions

This study develops a robust and comprehensive framework that integrates multiple advanced methodologies to address critical challenges in credit risk control [4]. The framework incorporates feature optimization through the enhanced Tree-Seed Algorithm, specifically the Modified Convergence-Adaptive Tree-Seed Algorithm (MCATSA), which significantly improves the efficiency of feature selection by mitigating issues such as premature convergence. Additionally, it employs spatiotemporal risk tracking using a macro-fused Deep Graph Neural Network (DGNN), which enables the precise identification and monitoring of risk patterns over time and across different spatial dimensions. Furthermore, the framework leverages automatic decision-making capabilities powered by Reinforcement Learning, which facilitates adaptive and intelligent responses to dynamic risk scenarios. Extensive multi-dimensional experiments validate the framework's effectiveness, demonstrating its superiority in optimizing credit risk management processes and achieving enhanced predictive accuracy. This innovative approach provides a significant contribution to the field by addressing key limitations in existing methodologies and offering a scalable solution for real-world applications.

2. Methodology

The full-process architecture of the IOA-DGNN-RL credit risk assessment system is employed to ensure a comprehensive and robust evaluation of credit risks, as illustrated in Figure 1. This advanced framework incorporates several key components that work in a synergistic manner. Multi-source data fusion is utilized to integrate diverse datasets, enabling a more holistic understanding of credit risk factors. Additionally, multi-strategy feature optimization, based on the MCATSA methodology, enhances the precision and relevance of the extracted features [5]. The DGNN spatiotemporal risk propagation modeling component captures dynamic risk patterns over time and space, providing deeper insights into risk behaviors. Finally, reinforcement learning is applied for dynamic decision-making, allowing the system to adapt to evolving scenarios, while multi-dimensional performance evaluation ensures the reliability and accuracy of the system's outputs.

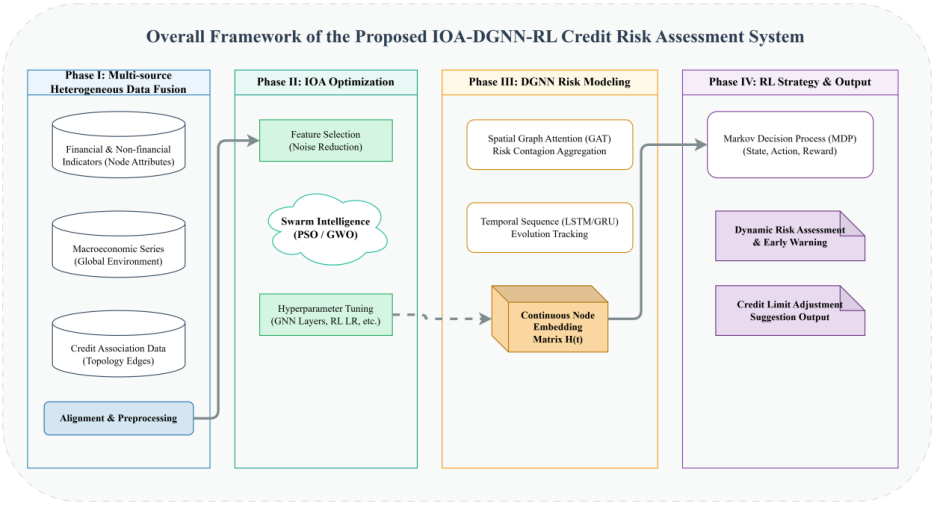

Figure 1. Overall Framework of the Ioa-dgnn-rl Credit Risk Assessment System

2.1. Data Fusion and Problem Formulation

The data utilized in this study are derived from the CSMAR Database, excluding ST and financial stocks, spanning the years 2021 to 2024. These data encompass corporate non-financial indicators, quantitative risk labels, and macroeconomic variables such as GDP, CPI, M2, and the risk-free interest rate. Following uniform encoding and temporal alignment, enterprises are represented as network nodes V, while supply chain and guarantee relationships are modeled as edges E. The primary objective of the risk identification task is to dynamically estimate the default probability of nodes within the network and to provide optimal credit decisions [6]. This is achieved by analyzing the combined effects of the dynamic credit graph $G = (V, E)$ and the macroeconomic vector. The methodology integrates multi-source data fusion to construct a dynamic credit network topology, as illustrated in Figure 2. This approach ensures a comprehensive evaluation of credit risks by leveraging interconnected enterprise relationships and macroeconomic trends, thereby enhancing the accuracy and reliability of credit decision-making processes.

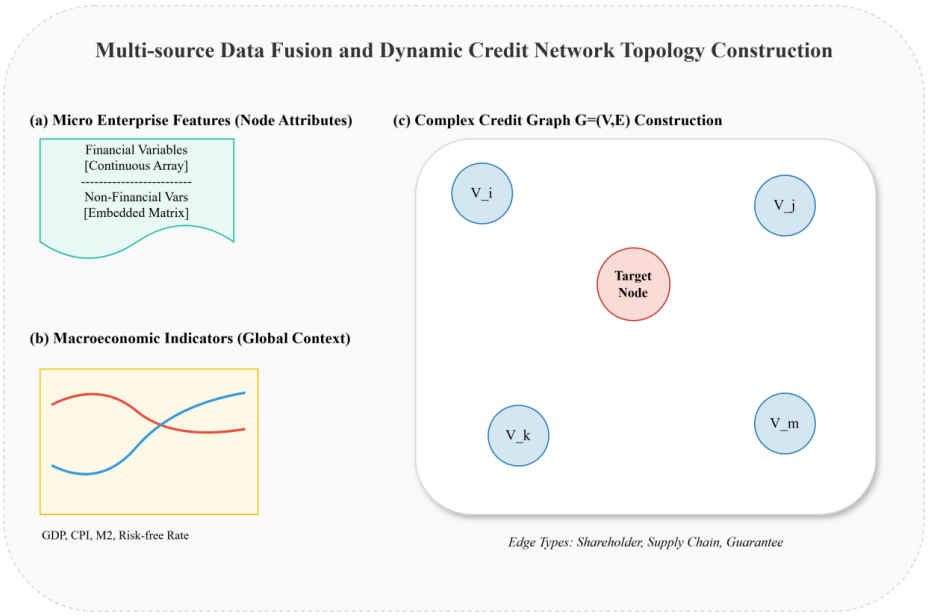

Figure 2. Multi-source Data Fusion and Dynamic Credit Network Topology Construction

2.2. Improved TSA for Feature Selection and Parameter Optimization

The standard TSA models the reproduction process of tree seeds, but its application in financial feature selection has shown limitations in terms of efficiency. The MCATSA introduced in this study functions as a meta-learning engine, with its fitness function designed to balance prediction performance metrics, such as AUC and KS, alongside a feature sparsity penalty. This dual focus ensures the elimination of noise while preserving critical features essential for effective risk control. To address the shortcomings of traditional algorithms, the MCATSA has been enhanced through five collaborative multi-strategy improvements [6]. These enhancements aim to optimize its performance by integrating advanced methodologies that improve convergence speed, enhance solution diversity, and refine feature selection accuracy. This approach ensures that the algorithm not only identifies high-value features but also maintains computational efficiency, making it a robust tool for financial data analysis and decision-making.

2.2.1. HTC Initialization

As illustrated in Figure 3, the introduction of Heterogeneous Tent-Logistic Chaos (HTC) initialization offers a significant improvement over traditional random mapping techniques. This method ensures a uniform distribution of the population across complex feature spaces, effectively mitigating the "clustering" phenomenon that often arises in conventional approaches. By addressing this issue, HTC initialization reduces the likelihood of significant search blind spots within the credit feature space [7]. This uniformity is particularly critical in enhancing the robustness and accuracy of feature exploration, as it provides a more comprehensive representation of the decision domain. Such advancements are essential for identifying subtle patterns and anomalies that may otherwise remain undetected in traditional methods.

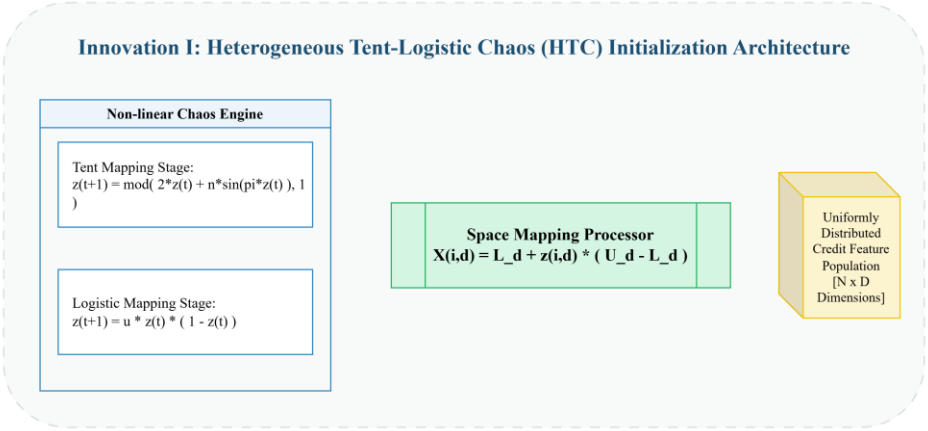

Figure 3. Heterogeneous Tent-Logistic Chaos (HTC) Initialization Architecture

The architecture of the HTC initialization method integrates a nonlinear chaotic engine, which operates through two interconnected stages: the tent map stage and the logistic map stage. The tent map stage is specifically designed to achieve global ergodicity, ensuring that the generated sequences exhibit high uniformity across the feature space. This characteristic is vital for maintaining a balanced exploration of the decision domain, as it prevents over-concentration in specific regions. The logistic map stage, on the other hand, introduces nonlinear complexity into the system, enhancing its ability to model intricate relationships within the data. Together, these stages form a cohesive framework that significantly improves the initialization process, enabling more effective feature space exploration.

In the tent mapping stage, the application of formula (1) ensures that the chaotic sequences generated exhibit global ergodicity and high uniformity. This property is crucial for achieving a comprehensive exploration of the feature space, as it minimizes the risk of over-sampling or under-sampling specific regions [8]. By leveraging the inherent

properties of the tent map, this stage lays a strong foundation for the subsequent processes, ensuring that the initialization process begins with a well-distributed population. Such uniformity is particularly important in scenarios where the feature space is highly complex or multidimensional, as it facilitates a more balanced and effective search process.

$$z(t+1) = mod(2z(t) + \eta sin(\pi z(t)),1) \quad (1)$$

The logistic mapping stage employs formula (2) to introduce nonlinear complexity into the chaotic sequences generated during the initialization process. This stage is designed to enhance the diversity of the population by incorporating intricate patterns and relationships that are representative of real-world data. The nonlinear nature of the logistic map ensures that the sequences generated are not only diverse but also capable of capturing subtle variations within the feature space. This added complexity is instrumental in improving the overall robustness of the initialization process, as it enables the system to adapt to a wide range of scenarios and challenges.

$$z(t+1) = \mu z(t)(1 - z(t)) \quad (2)$$

The chaotic sequences generated through the tent and logistic mapping stages are further processed by a spatial mapping processor, which utilizes formula (3) to map individuals into the decision domain. This mechanism ensures that the population is uniformly distributed across the credit feature groups, providing a solid topological foundation for the analysis. By achieving this uniform distribution, the system is better equipped to identify rare but critical default risk scenarios that may otherwise go unnoticed. The spatial mapping processor plays a pivotal role in bridging the gap between chaotic sequence generation and practical application, ensuring that the initialization process is both effective and efficient in addressing complex decision-making challenges [9].

$$X(i,d) = L_d + z(i,d) \cdot (U_d - L_d) \quad (3)$$

2.2.2. Fldra Resource Dynamic Allocation

As illustrated in Figure 4, the Fitness-Driven Layered Resource Allocation (FLDRA) system is designed to emulate a hierarchical biological structure, effectively categorizing the population into three distinct levels based on real-time fitness rankings. These levels include the elite level, which comprises the top 5% of individuals demonstrating superior fitness, the general level representing the majority of the population, and the stagnant level, which includes individuals with minimal progress or adaptation [10]. This stratification enables a more targeted allocation of resources, ensuring that computational efforts are concentrated on individuals with the highest potential for contributing to the system's objectives. By prioritizing the elite level, the FLDRA system enhances the efficiency of resource utilization, fostering rapid advancements in identifying critical nodes within complex networks. Furthermore, this layered approach mitigates the risk of resource wastage by systematically reducing allocation to less promising individuals, thereby optimizing the overall performance of the model.

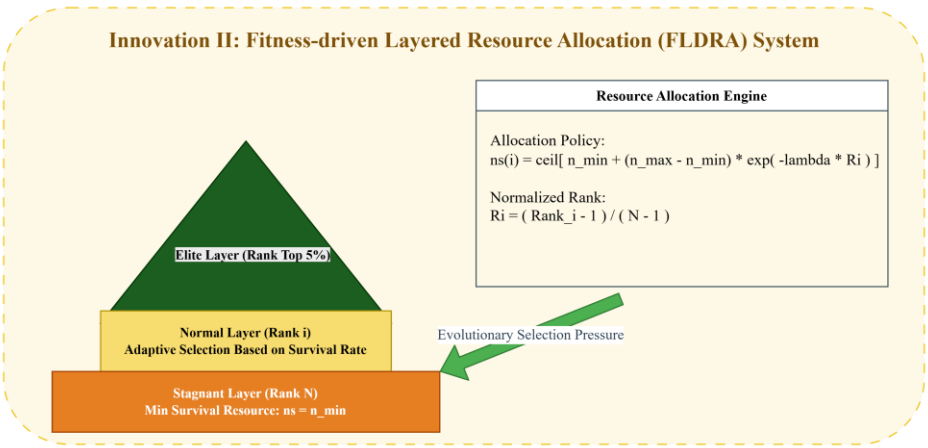

Figure 4. Fitness-driven Layered Resource Allocation (Fldra) System

The resource allocation engine within the FLDRA framework employs a specialized strategy to maximize efficiency and precision. As depicted in formula (4), normalized rankings are utilized to determine the distribution of resources, with individuals exhibiting higher fitness—those positioned closer to the risk centroid—receiving the maximum seed quota for intensive development. This approach ensures that computational resources are strategically directed towards individuals with the greatest potential for uncovering hidden risk nodes within expansive credit networks [11]. By applying evolutionary selection pressure, the system dynamically adjusts resource flow, favoring high-potential individuals while simultaneously maintaining a balance across the population. This mechanism significantly enhances the model's accuracy and reliability, enabling it to pinpoint critical risk nodes with greater precision. The integration of this strategy within the FLDRA framework underscores its capability to adapt to complex scenarios, ensuring robust performance in diverse applications.

$$n_s(i) = \text{ceil}[n_{\min} + (n_{\max} - n_{\min})\exp(-\lambda R_i)] \quad (4)$$

2.2.3. Sigmoid-Cosine Energy Modulation

As illustrated in Figure 5, the primary innovation of MCATSA lies in its ability to dynamically adjust the balance between exploration and exploitation through the application of the Sigmoid-Cosine energy strategy. This approach ensures that the algorithm can effectively navigate complex optimization landscapes by modulating energy levels in a controlled manner. The Sigmoid-Cosine strategy introduces a non-linear mechanism that enhances the adaptability of the algorithm, allowing it to respond to varying computational demands during different phases of the optimization process. By leveraging this strategy, the system achieves a more efficient transition between the global exploration phase and the local exploitation phase, ultimately improving the overall performance and robustness of the algorithm.

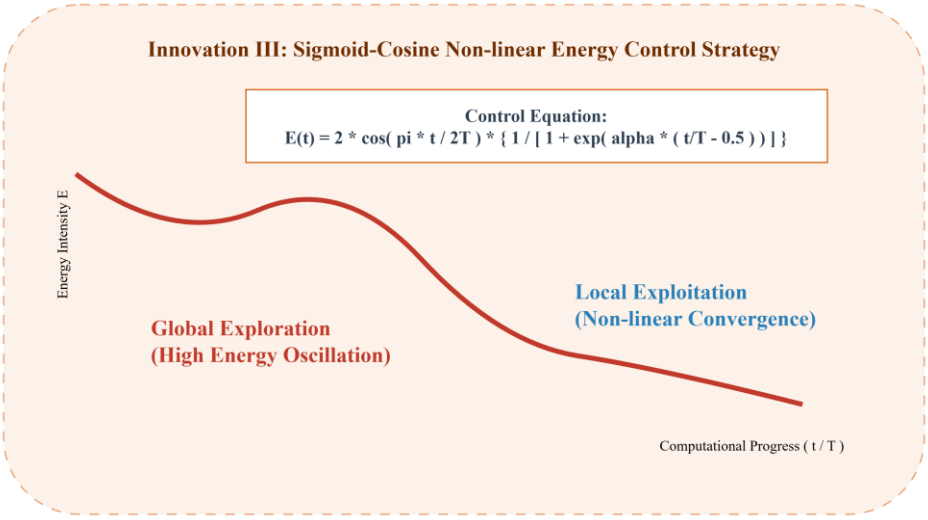

Figure 5. Sigmoid-Cosine Non-linear Energy Control Strategy

The energy factor E(t), as depicted in Figure 5, plays a pivotal role as a regulatory component within the algorithm. Governed by formula $E(t) = 2\cos\left(\frac{\pi t}{2T}\right) \cdot \left\{\frac{1}{1+\exp\left(\alpha\left(\frac{t}{T}-0.5\right)\right)}\right\}$, this factor is designed to facilitate a seamless shift between the global exploration and local exploitation phases. During the initial global exploration phase, the energy factor exhibits high oscillatory behavior, enabling agents to traverse diverse potential surfaces and avoid becoming trapped in suboptimal solutions. As the computation advances, the energy factor undergoes a controlled decay, guided by the Sigmoid function. This decay introduces a damping effect that gradually reduces the energy levels, steering the algorithm into the local exploitation phase. This phase is

characterized by a focus on fine-grained optimization, where the system converges non-linearly toward optimal solutions. The Sigmoid-Cosine strategy ensures a smooth and efficient transition between these phases, enhancing the algorithm's ability to balance exploration and exploitation effectively.

2.2.4. SDMC Collaborative Modal Strategy

As illustrated in Figure 6, a dual-mode switching mechanism has been developed to address the prevalent issue of collinearity in financial data analysis. This mechanism integrates sine-cosine perturbation with differential collaboration, forming a "dual-wheel drive" strategy. The sine-cosine perturbation introduces dynamic adjustments to the search trajectory, effectively disrupting the coupling relationships between features. Meanwhile, the differential collaboration enhances the precision of feature selection by leveraging vector-based differences. Together, these two modes work synergistically to identify the optimal subset of features with high accuracy, thereby improving the robustness and reliability of financial data modeling. This innovative approach not only mitigates the risks associated with feature interdependence but also ensures a more comprehensive exploration of the feature space, ultimately leading to superior analytical outcomes.

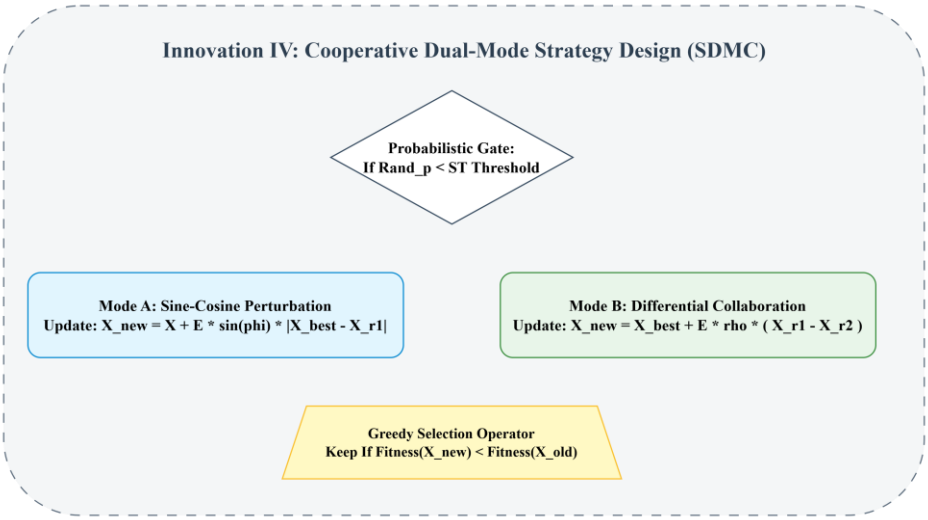

Figure 6. Cooperative Dual-Mode Strategy Design (SDMC)

Mode A, referred to as sine-cosine perturbation, employs a triangular phase mechanism to dynamically alter the search trajectory [12]. This approach is particularly effective in breaking the coupling relationships between features, which often hinder the identification of optimal subsets. By introducing controlled perturbations, Mode A ensures that the search process avoids local optima and explores a broader solution space. The mathematical foundation of this mode is encapsulated in formula (6), which defines the sine-cosine adjustments applied to the feature set. This targeted perturbation strategy enhances the adaptability and efficiency of the feature selection process, making it a critical component of the dual-mode mechanism.

$$X_{\text{new}} = X + E \cdot \sin(\phi) \cdot |X_{\text{best}} - X_{r1}| \quad (6)$$

Mode B, known as differential cooperation, focuses on precise neighborhood searches by utilizing vector-based differences. This mode is designed to refine the search process by systematically evaluating the variations between feature vectors, as outlined in formula (7). By concentrating on localized adjustments, Mode B ensures that the feature selection process is both accurate and efficient. This method complements the broader exploratory capabilities of Mode A, creating a balanced approach that combines global exploration with local refinement. The integration of these two modes within the dual-mode strategy significantly enhances the overall effectiveness of feature selection, particularly in complex financial datasets where precision is paramount.

$$X_{\text{new}} = X_{\text{best}} + E \cdot \rho \cdot (X_{r1} - X_{r2}) \quad (7)$$

2.2.5. CGM Stagnation Wake-Up Mechanism

To ensure the robustness of the model when confronted with unpredictable "black swan" events that may lead to convergence at local optima, the Cauchy-Gaussian Mixture (CGM) mutation mechanism has been introduced, as illustrated in Figure 7. This mechanism is designed to enhance the adaptability and resilience of the algorithm by addressing stagnation scenarios effectively. By incorporating this approach, the model gains the ability to navigate complex optimization landscapes, avoiding pitfalls that could compromise its performance. The CGM mechanism leverages the complementary strengths of Cauchy and Gaussian distributions, ensuring a balanced strategy for overcoming stagnation and maintaining the integrity of the evolutionary process [13].

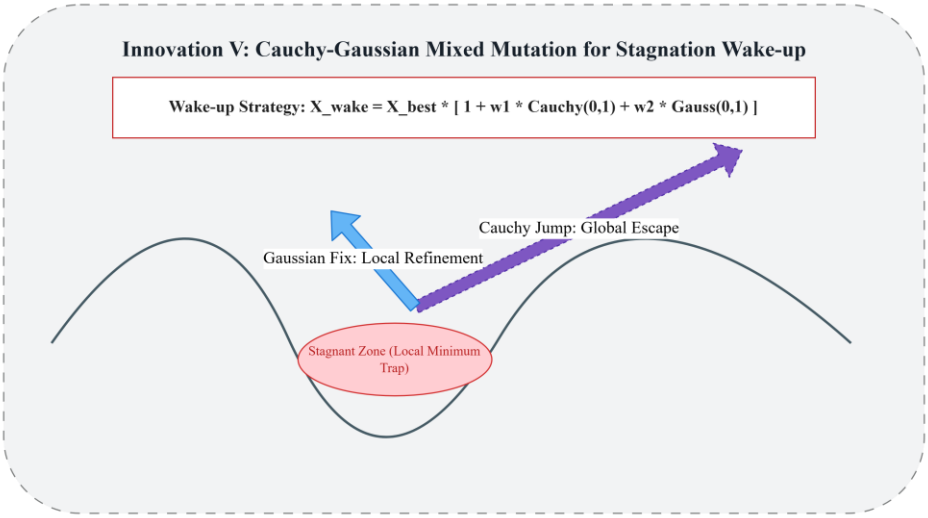

Figure 7. Cauchy-Gaussian Mixed Mutation for Stagnation Wake-up

When the population encounters a stagnant region, often referred to as a local minimum trap, a hybrid awakening strategy is activated, as demonstrated in formula (8). This dual-action mechanism combines two distinct perturbation methods: Cauchy jumps and Gaussian fixation. The Cauchy jumps utilize heavy-tailed characteristics to enable long-distance displacement, facilitating global escape from deceptive regions. Meanwhile, Gaussian fixation focuses on local refinement, ensuring precision in optimization. Together, these perturbations provide the algorithm with a "quantum jump" capability, allowing it to restart the evolutionary process effectively. This capability is particularly vital for maintaining prediction reliability in dynamic and fluctuating environments, such as financial markets. By integrating this hybrid strategy, the algorithm achieves a robust balance between exploration and exploitation, ensuring its ability to adapt to complex scenarios and sustain long-term performance.

$$X_{\text{wake}} = X_{\text{best}} \cdot [1 + w_1 \text{Cauchy}(0,1) + w_2 \text{Gauss}(0,1)] \quad (8)$$

2.3. DGNN-based Risk Propagation Model

In the spatial dimension, advanced graph-based neural networks such as GraphSAGE and GAT are employed to aggregate and analyze the risk characteristics of interconnected nodes, which represent associated enterprises. This approach enables the model to capture intricate relationships and dependencies within the network. In the temporal dimension, Long Short-Term Memory (LSTM) networks are utilized to process the sequential evolution of feature data over time, ensuring that temporal patterns and trends are effectively captured. Additionally, a macroeconomic vector is integrated into the network as a global contextual factor, allowing the model to account for the influence of broader macroeconomic cycles on the dynamics of risk contagion [14]. This

comprehensive framework enhances the model's ability to simulate and predict risk propagation with greater accuracy and reliability.

2.4. RL-based Risk Decision

The reinforcement learning module illustrated in Figure 8 utilizes the risk embedding generated by DGNN as the state representation. This approach enables the system to dynamically adapt to varying risk scenarios by defining actions such as adjusting credit limits or initiating alerts. The reward function is meticulously designed to optimize the balance between accurate predictions and the penalties associated with false positives and negatives. By maximizing the expected value of these outcomes, the framework ensures intelligent decision-making that evolves in response to real-time data. This dynamic methodology enhances the system's ability to address complex risk management challenges, providing a robust mechanism for maintaining operational stability and improving predictive accuracy in diverse financial environments.

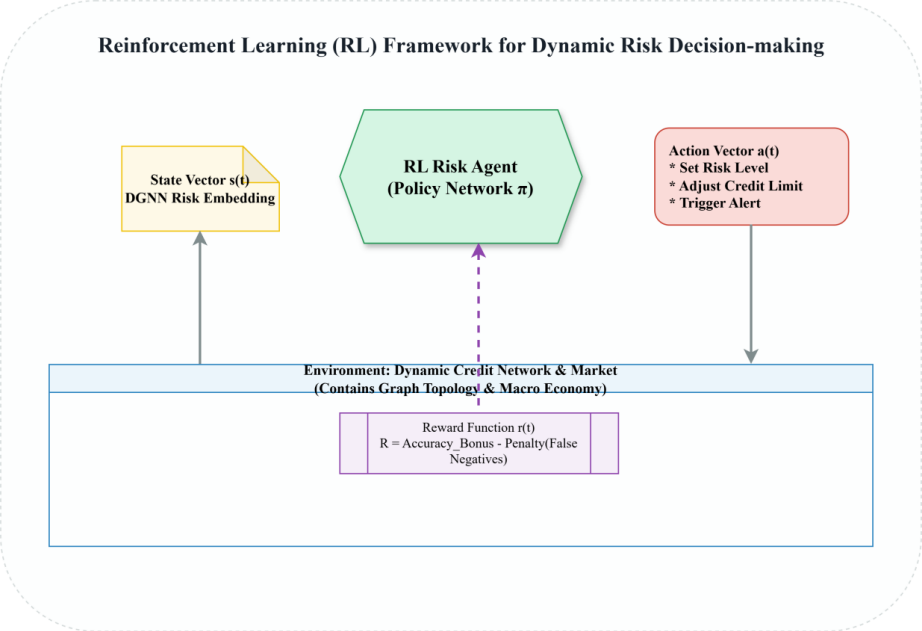

Figure 8. Reinforcement Learning (RL) Framework for Dynamic Risk Decision-making

3. Experimental Verification of Improved TSA

3.1. Benchmark Functions

To scientifically verify the fundamental optimization capability and universality of MCATSA, this study conducted a rigorous evaluation using a comprehensive set of standard continuous optimization benchmark functions. These benchmark functions are specifically designed to test different aspects of algorithm performance. The test set includes unimodal functions, which are utilized to evaluate the algorithm's ability to refine solutions within a localized search space, thereby assessing its local optimization capability. Additionally, multimodal functions are incorporated to examine the algorithm's proficiency in exploring diverse regions of the search space, which is critical for global optimization. The detailed characteristics and mathematical formulations of these benchmark functions are presented in Table 1, ensuring clarity and reproducibility of the experimental setup. By employing this diverse set of functions, the study aims to provide a robust and unbiased assessment of MCATSA's optimization performance across varying problem complexities.

Table 1. Benchmark Test Function

Type	Function	Mathematical Formulation	Search Range
Unimodal	Sphere	$f_1(x)=\sum_{i=1}^{D} x_i^2$	[-100,100]
	Rosenbrock	$f_2(x)=\sum_{i=1}^{D-1}[100(x_{i+1}-x_i^2)^2+(x_i-1)^2]$	[-30,30]
	Step	$f_3(x)=\sum_{i=1}^{D}(\lfloor x_i+0.5\rfloor)^2$	[-100,100]
Multimodal	Rastrigin	$f_4(x)=\sum_{i=1}^{D}[x_i^2-10\cos(2\pi x_i)+10]$	[-5.12,5.12]
	Ackley	$f_5(x)=-20\exp(-0.2\sqrt{\frac{1}{D}}$	[-32,32]
	Griewank	$f_6(x)=\frac{1}{4000}\sum_{i=1}^{D} x_i^2-\prod_{i=1}^{D}\cos(\frac{x_i}{\sqrt{i}})+1$	[-600,600]

In terms of parameter configuration, the experimental setup was carefully designed to ensure statistical reliability and meaningful comparisons. The population size for the algorithm was set to 30, which balances computational efficiency and solution diversity. Furthermore, the maximum number of iterations was limited to 100, providing sufficient opportunities for convergence while avoiding excessive computational overhead. To enhance the robustness of the results, 30 independent experiments were conducted for each benchmark function. The mean and standard deviation of the outcomes were calculated to provide a comprehensive statistical analysis of the algorithm's performance. These results, summarized in Table 2, offer valuable insights into the consistency and reliability of the improved TSA under varying experimental conditions. Such meticulous parameter settings and statistical evaluations underscore the scientific rigor of this study [15].

Table 2. Improve TSA Parameter Setting

Parameter	Meaning	Value
N	Population size	30
Tmax	Maximum iterations	100
pm	Mixed mutation probability	0.10
ϱ	Elite retention ratio	0.20
λ	Penalty coefficient	0.50
α	Energy adjustment factor	1.20
Initialization	Tent-Logistic chaotic initialization	Tent-Logistic chaotic initialization
Boundary handling	Reflection mapping repair	Reflection mapping repair

3.2. Convergence Analysis

As illustrated in Figure 9, a comparative analysis of the convergence curves was performed between MCATSA and several classical heuristic algorithms, including the Tree-Structured Search Algorithm (TSA), Particle Swarm Optimization (PSO), Grey Wolf Optimization (GWO), Genetic Algorithm (GA), and Butterfly Optimization Algorithm (BOA). This comparison highlights the relative performance of these algorithms in terms of optimization efficiency and convergence behavior [16]. The visualization provided by Figure 9 serves as a critical tool for understanding the dynamics of these algorithms across benchmark functions, offering insights into their strengths and limitations in diverse optimization scenarios.

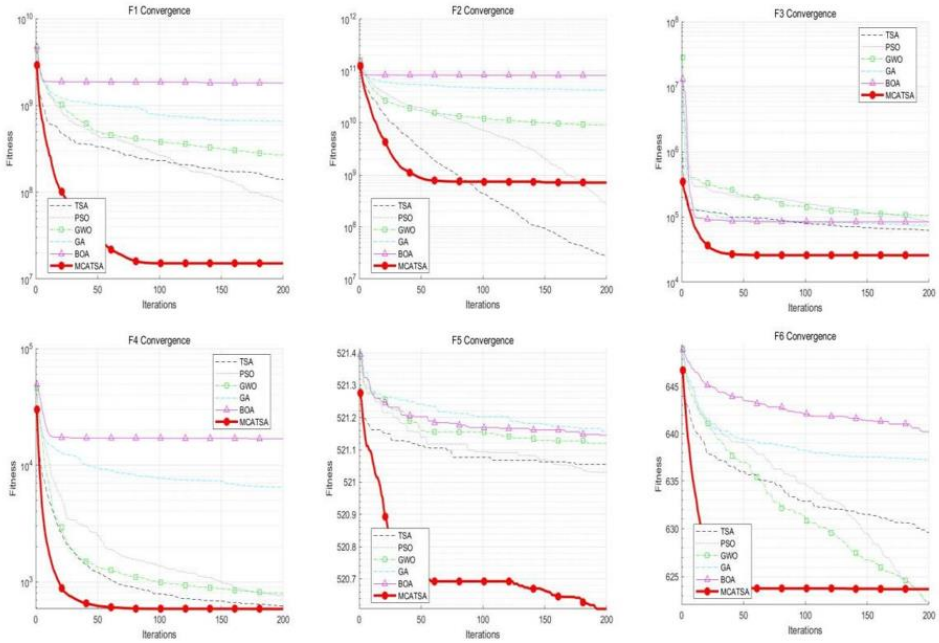

Figure 9. Convergence Curves of Mcatsa and Classical Heuristic Algorithms on Benchmark Functions F1--F6.

The convergence results depicted in Figure 9 reveal that MCATSA demonstrates a notably steep downward trajectory during the initial iteration phase, underscoring its robust capability for rapid initial positioning. This characteristic is particularly advantageous in scenarios requiring swift identification of optimal solutions. Furthermore, in the intermediate and later stages of iteration, the algorithm leverages its non-linear energy adjustment mechanism to effectively mitigate the risk of premature convergence. This adaptive feature enables MCATSA to maintain high optimization accuracy, outperforming other heuristic algorithms in terms of precision and reliability. The algorithm's ability to balance exploration and exploitation throughout the optimization process ensures its superiority in handling complex benchmark functions [17].

3.3. Rank First Statistics

As illustrated in Figure 10, the "Top Rank Statistics" derived from the outcomes of 30 independent experiments integrates the average performance metrics achieved by each algorithm. The statistical analysis reveals that MCATSA consistently outperforms other algorithms, securing the highest rank across a majority of the test functions. This dominance underscores the algorithm's superior design and optimization capabilities, which enable it to excel in diverse computational scenarios. The robustness of MCATSA is further highlighted by its ability to maintain top-tier performance under varying experimental conditions, demonstrating its adaptability and reliability in solving complex optimization problems.

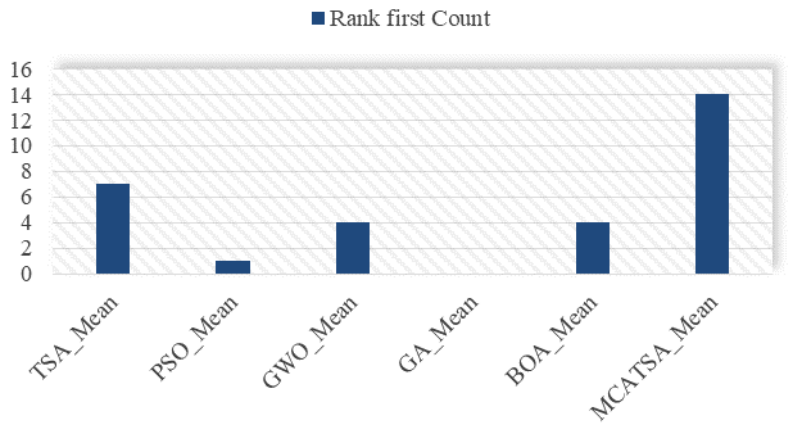

Figure 10. Rank First Count Statistics

As depicted in Figure 11, the data distribution characteristics presented through Box plots provide valuable insights into the comparative performance of MCATSA and other heuristic algorithms. The analysis reveals that MCATSA exhibits an exceptionally low lower bound for optimization, indicating its ability to achieve highly efficient solutions. Furthermore, the algorithm demonstrates a remarkably small variance, which serves as compelling evidence of its architectural enhancements contributing to outstanding overall robustness. These findings confirm that MCATSA is not only effective in achieving optimal results but also consistent in its performance across benchmark functions F1-F6, making it a reliable choice for tackling a wide range of optimization challenges.

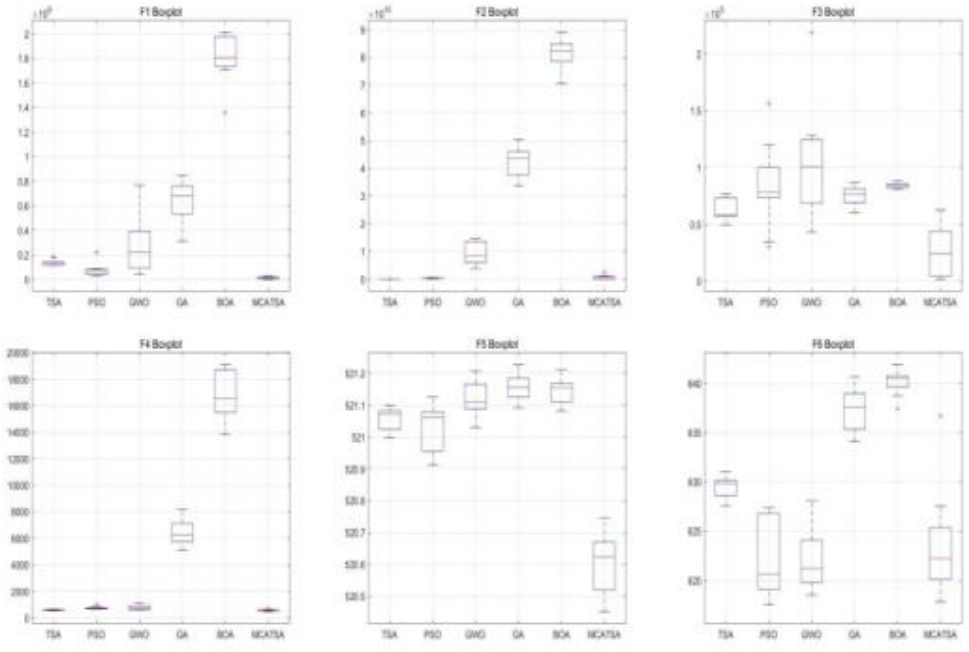

Figure 11. Box Plot Comparison of Mcatsa and Other Heuristic Algorithms on Benchmark Functions F1--F6.

3.4. Feature Selection Results

As demonstrated in Table 3, the MCATSA algorithm exhibits superior performance in the domain of credit feature selection when compared to other methods. By reducing the feature dimensions to only 12, it achieves enhanced classification metrics, including higher AUC and KS values on the validation dataset [11]. This improvement underscores

its effectiveness as a feature selection tool, particularly for optimizing subsequent predictive models. The streamlined dimensionality not only reduces computational complexity but also enhances model interpretability, making it a valuable approach for applications requiring efficient and accurate feature selection. Table 3 provides a detailed comparison of the results obtained using various intelligent algorithms, further highlighting the advantages of MCATSA in achieving robust and reliable outcomes in feature selection tasks.

Table 3. Comparison of Feature Selection Results Based on Different Intelligent Algorithms

Method	Number of Selected Features	Validation AUC	Validation KS	Training Time (s)
All Features	28	0.881	0.593	71.4
Original TSA	15	0.887	0.601	64.8
PSO	18	0.879	0.588	61.2
GWO	16	0.884	0.596	62.5
Improved TSA	12	0.896	0.616	66.1

4. Experimental Results

4.1. Experimental Setup

This experiment utilizes credit data from non-financial enterprises extracted from the CSMAR database, with ST stocks and financial stocks excluded, resulting in a dataset comprising 5,403 entries. The dataset is meticulously divided into training, validation, and test sets, adhering to a chronological order and maintaining a ratio of approximately 7:1:2. The evaluation framework incorporates key financial risk control metrics, including AUC, KS value, precision, recall, and F1-Score, to ensure a comprehensive assessment of the model's ability to identify default risks and facilitate accurate credit decision-making. To establish a fair and comparative experimental environment, the proposed IOA-DGNN-RL framework is benchmarked against several baseline models, including logistic regression, XGBoost, long short-term memory networks, graph attention networks, and dynamic graph neural networks. The parameter settings for the MCATSA optimization module are carefully configured, with a population size of 30 and a maximum of 100 iterations. Additionally, a mixed mutation probability of 0.10 and an elite retention ratio of 0.20 are employed to optimize performance across all models under consistent hyperparameter conditions. This rigorous setup ensures that the experimental results are both reliable and reproducible, providing valuable insights into the comparative effectiveness of the proposed framework in addressing financial risk challenges. The methodology underscores the importance of robust data partitioning and parameter tuning in achieving optimal model performance.

4.2. Comparative Results

The proposed comprehensive framework, IOA-DGNN-RL, was rigorously evaluated against a machine learning baseline model using the test set. The results, as presented in Table 4, demonstrate that IOA-DGNN-RL achieved superior performance, with an AUC of 0.901. This outcome underscores the effectiveness of the collaborative optimization strategy that integrates dynamic graph networks with reinforcement learning. The high AUC value indicates a robust ability to distinguish between different classes, which is critical for accurate credit risk prediction [11]. Furthermore, the framework's design allows it to adapt dynamically to complex data structures, ensuring enhanced predictive accuracy. These findings highlight the potential of advanced machine learning techniques in addressing challenges in financial risk assessment.

Table 4. Overall Credit Risk Prediction Performance Results

Model	AUC	KS	Precision	Recall	F1
LR	0.782	0.461	0.703	0.548	0.617
XGBoost	0.843	0.529	0.732	0.631	0.678
LSTM	0.825	0.518	0.719	0.617	0.664
GAT	0.859	0.553	0.744	0.648	0.692
DGNN	0.875	0.579	0.761	0.671	0.713
IOA-DGNN	0.887	0.605	0.773	0.689	0.728
IOA-DGNN-RL	0.901	0.627	0.789	0.706	0.745

4.3. Ablation Study

As demonstrated in Table 5, the ablation experiment analysis underscores the critical role of each module in the overall model performance. When the network topology module is excluded (w/o Network), the AUC metric experiences a significant drop to 0.855. This result highlights the indispensable nature of modeling the spatial risk contagion mechanism, which is essential for effective credit risk control [13]. Similarly, the removal of the MCATSA module or macro features also leads to a marked reduction in model accuracy, further emphasizing their importance. The findings suggest that the integration of feature selection, dynamic graph propagation, and reinforcement learning decision-making creates a synergistic effect that enhances the model's predictive capabilities. The ablation study thus validates the necessity of each component, demonstrating that their combined contributions are greater than the sum of their individual effects, particularly in addressing complex risk assessment scenarios.

Table 5. Ablation Experiment Results

Variant	AUC	KS	Precision	Recall	F1
Full model (IOA-DGNN-RL)	0.901	0.627	0.789	0.706	0.745
w/o IOA	0.887	0.608	0.776	0.689	0.731
w/o DGNN	0.862	0.571	0.752	0.652	0.702
w/o RL	0.893	0.615	0.781	0.697	0.736
w/o Macro	0.874	0.589	0.760	0.668	0.716
w/o Network	0.855	0.560	0.744	0.640	0.691

5. Conclusion

The IOA-DGNN-RL framework developed in this study introduces a groundbreaking approach to dynamic credit risk assessment by integrating advanced computational methodologies. The innovative MCATSA algorithm addresses critical challenges in traditional optimization processes, offering robust solutions for data denoising and hyperparameter tuning. By leveraging dynamic graph networks in conjunction with reinforcement learning, the framework effectively captures the intricate spatiotemporal contagion pathways of financial risks, enabling a seamless transition from predictive analytics to actionable decision-making. This closed-loop system enhances the precision and adaptability of risk management strategies, particularly in complex financial environments. Future research directions will delve deeper into the structural evolution of multi-layer heterogeneous financial networks, aiming to uncover hidden interdependencies and systemic vulnerabilities. Additionally, efforts will be directed toward improving the interpretability of graph-based models, ensuring their practical applicability in diverse financial scenarios and fostering trust among stakeholders in high-stakes decision-making processes.

References

1. S. Mirjalili and A. Lewis, "The whale optimization algorithm," *Advances in Engineering Software*, vol. 95, pp. 51-67, 2016.

2. M. S. Kiran and H. Hakli, "A tree–seed algorithm based on intelligent search mechanisms for continuous optimization," *Applied Soft Computing*, vol. 98, p. 106938, 2021.
3. J. Kennedy and R. Eberhart, "Particle swarm optimization," in *Proceedings of ICNN'95-International Conference on Neural Networks*, vol. 4, pp. 1942-1948, Nov. 1995.
4. A. Sozen, E. Arcaklioglu, and M. Ozkaymak, "Modelling of Turkey's net energy consumption using artificial neural network," *International Journal of Computer Applications in Technology*, vol. 22, no. 2-3, pp. 130-136, 2005.
5. H. Xu, R. Li, and Q. Chen, "Research on Deep Neural Network Hyperparameter Optimization Method Based on Improved Tree Seed Algorithm," in *2025 IEEE 7th International Conference on Communications, Information System and Computer Engineering (CISCE)*, pp. 919-922, May 2025.
6. F. S. Gharehchopogh, "Advances in tree seed algorithm: A comprehensive survey," *Archives of Computational Methods in Engineering*, vol. 29, no. 5, pp. 3281-3304, 2022.
7. J. S. Alzahrani et al., "Tree seed algorithm-based feature selection with optimal deep learning model for supply chain management," *Fluctuation and Noise Letters*, vol. 23, no. 2, p. 2440019, 2024.
8. A. C. Cinar, "Training feed-forward multi-layer perceptron artificial neural networks with a tree-seed algorithm," *Arabian Journal for Science and Engineering*, vol. 45, no. 12, pp. 10915-10938, 2020.
9. J. Liu, Y. Hou, Y. Li, and H. Zhou, "A multi-strategy improved tree–seed algorithm for numerical optimization and engineering optimization problems," *Scientific Reports*, vol. 13, no. 1, p. 10768, 2023.
10. J. Jiang et al., "DTSA: Dynamic tree-seed algorithm with velocity-driven seed generation and count-based adaptive strategies," *Symmetry*, vol. 16, no. 7, p. 795, 2024.
11. S. T. Amin, "Tree Seed Algorithm-Based Optimized Deep Features Selection for Glaucoma Disease Classification," *International Journal of Advanced Computer Science & Applications*, vol. 16, no. 3, 2025.
12. Q. Zhou, R. Dai, G. Zhou, S. Ma, and S. Luo, "An Enhanced Tree-Seed Algorithm for Function Optimization and Production Optimization," *Biomimetics*, vol. 9, no. 6, p. 334, 2024.
13. A. Beşkirli, D. Özdemir, and H. Temurtaş, "A comparison of modified tree–seed algorithm for high-dimensional numerical functions," *Neural Computing and Applications*, vol. 32, no. 11, pp. 6877-6911, 2020.
14. Z. Qiao, L. Wu, A. A. Heidari, X. Zhao, and H. Chen, "An enhanced tree-seed algorithm for global optimization and neural architecture search optimization in medical image segmentation," *Biomedical Signal Processing and Control*, vol. 104, p. 107457, 2025.
15. S. Zhao, N. Wang, and X. Liu, "Artificial bee colony algorithm with tree-seed searching for modeling multivariable systems using GRNN," in *2019 Chinese Control and Decision Conference (CCDC)*, pp. 4702-4707, June 2019.
16. I. Katib, E. Albassam, S. A. Sharaf, and M. Ragab, "Harnessing probabilistic neural network with triple tree seed algorithm-based smart enterprise quantitative risk management framework," *Scientific Reports*, vol. 14, no. 1, p. 22293, 2024.
17. M. F. Aslan, K. Sabanci, and E. Ropelewska, "A new approach to COVID-19 detection: An ANN proposal optimized through tree-seed algorithm," *Symmetry*, vol. 14, no. 7, p. 1310, 2022.

Disclaimer/Publisher's Note: The statements, opinions and data contained in all publications are solely those of the individual author(s) and contributor(s) and not of Publisher and/or the editor(s). Publisher and/or the editor(s) disclaim responsibility for any injury to people or property resulting from any ideas, methods, instructions or products referred to in the content.